On the Scalability of Constructive Interference in Low-Power Wireless Networks

Claro A. Noda[1,2], Carlos M. Pérez-Penichet[2], Balint Seeber[3], Marco Zennaro[4], Mário Alves[1], and Adriano Moreira[2]

[1] CISTER/INESC-TEC, Polytechnic Institute of Porto (ISEP/IPP), Portugal
{candz,mjf}@isep.ipp.pt
[2] Algoritmi Research Centre, University of Minho, Guimarães, Portugal
{cpp,adriano}@dsi.uminho.pt
[3] Ettus Research, Santa Clara, USA
balint.seeber@ettus.com
[4] Guglielmo Marconi Laboratory, ICTP, Trieste, Italy
mzennaro@ictp.it

Abstract. Constructive baseband interference has been recently introduced in low-power wireless networks as a promising technique enabling low-latency network flooding and sub-μs time synchronisation among network nodes. The scalability of this technique has been questioned in regards to the maximum temporal misalignment among baseband signals, due to the variety of path delays in the network. By contrast, we find that the scalability is compromised, in the first place, by emerging fast fading in the composite channel, which originates in the carrier frequency disparity of the participating repeaters nodes. We investigate the multisource wave problem and show the resulting signal becomes vulnerable in the presence of noise, leading to significant deterioration of the link whenever the carriers have similar amplitudes.

1 Background and Related Work

Constructive Baseband Interference (CBI) exploits the spatial, temporal and spectral diversity exhibited by the wireless channel to introduce link redundancy and increase reliability. This diversity of the wireless channel manifests itself as a given symbol stream reaches across different wireless channels simultaneously and each symbol is unlikely to suffer the same level of distortion, small-scale multipath fading and attenuation in all channels at the same time. Therefore, concurrent transmission of identical packets from several senders can increase the quality of the wireless link towards a receiver.

CBI has been recently introduced in wireless networks by Rahul et al. [15]. Dutta et al. employed CBI to alleviate the acknowledgement implosion problem, using simultaneous transmissions of short acknowledgement packets, in a receiver-initiated low-power Medium Access Control (MAC) protocol [6]. Ferrari et al. devised a communication primitive for low-latency network flooding and sub-μs time synchronization for low-power wireless nodes [9]. In following works, Ferrari et al. also proposed an infrastructure (analogous to a shared bus), which supports mobile nodes in a multihop low-power wireless network [8]. Doddavenkatappa et al. further optimise network flooding enabling a multichannel packet pipeline across the network [3,4].

However, some limitations in the efficacy and scalability of CBI have been studied by Wang et al. [17]. They investigate the worst case scenario in a multihop network

T. Abdelzaher et al. (Eds.): EWSN 2015, LNCS 8965, pp. 250–257, 2015.

showing that cumulative non-deterministic delays in the system cause the temporal displacement between concurrent transmissions to exceed the symbol boundaries, leading to poor packet reception rate. We take a different perspective on this matter by analysing the superposition of carrier waves. The main contribution of this paper is that the scalability of CBI is not only limited by the variety of temporal delays as investigated by Wang et al. but, firstly, by specific properties of the composite signal.

The scalability of CBI is relevant because the disposition of wireless sensor nodes in a deployment should follow application needs. Consider the plausible scenario where a large number of fixed sensor nodes may be required in a given location, while sparse nodes suffice in other areas. Also mobile sensors attached to humans, animals or robots impose a dynamic spatial density. In such scenarios, bulk data transfer with high-throughput, low-latency and low-power are important system features. For example, the time window to transfer data might be limited in railway-bridge monitoring, as data is uploaded to passing trains [2]. CBI enhances link performance, radio coverage and enables node mobility. Nevertheless, we reveal a critical lack of link quality scalability with the number of concurrent repeaters.

We present the multisource wave problem (Section 2) and investigate the error rate and the envelope of the composite signal, which results from the superposition of all repeater signals. Our experiments (described in Section 3) show an acute signal vulnerability in the presence of noise and the consequent deterioration of the link quality for a power imbalance among two or more repeater signals smaller than 5 dB (Section 4). We discuss the results and reach conclusions in Section 5.

2 Constructive Interference

Constructive Baseband Interference occurs when multiple-source carriers, modulated with identical information and adequate time synchronization, add up in the receiver antenna. The time synchronization error plus the wave propagation delay difference among these signals must remain within symbol boundaries, to avoid intersymbol interference [5]. In the case of the IEEE 802.15.4 physical layer (PHY), half the symbol time corresponds to 0.5 µs [6,9].

Since the modulated carrier of each transmitter traverses distinct wireless channels towards the receiver, we refer to them as *individual channels* as they are, in general, statistically independent. Furthermore, the composite signal that results from the superposition of waves can be interpreted as if it traverses a *composite channel* characterised by the resulting sum of multisource carriers, in addition to the overall multipath effect of the individual channels.

2.1 Carrier Waves

Let us now look into wave properties to understand CBI. Without losing generality, we restrict this analysis to unmodulated carriers. The reader is referred to [17] for a detailed discussion on the baseband signal and carrier modulation. Let the composite unmodulated signal A_c from n sources be expressed as:

$$A_c = \sum_{i=1}^{n} A_i \sin(w_i t + \phi_i) \tag{1}$$

Also let A_i, w_i and ϕ_i represent the amplitude, angular frequency and phase of the individual sources respectively. Note that the multisource problem in equation (1) is similar to the multipath problem, where all frequencies are equal since they originate at a single source. On the other hand, multiple sources implies small disparities in the carrier frequencies, as there is always a limit in the frequency accuracy of the quartz-crystal based oscillators used to synthesize the carrier. Section 2.2 elaborates on this.

The properties of the probability density function (*pdf*) of the resultant amplitude or envelope of equation (1) are important for the performance evaluation of wireless systems. The modelling of fading and shadowing in the multipath problem (all w_i are equal) has been widely studied and an expression for the *pdf* can be found in [18].

To the best of our knowledge, an exact expression for the *pdf* of the envelope in equation (1) remains an open mathematical problem. Thus, for the sake of simplicity, let us consider the case of two sources ($n = 2$). Let the envelope E_c of equation (1) be:

$$E_c = \left[A_1^2 + A_2^2 + 2A_1A_2\cos\left(\left(\omega_1 - \omega_2\right)t + \varphi\right)\right]^{1/2} \tag{2}$$

Equation (2) reveals a harmonic function with angular frequency $w_c = w_1 - w_2$ which leads to periodic depressions in the amplitude of the composite signal. This is known as the beating effect. It is important to note that these depressions can be quite numerous during the packet duration, depending on w_c. As the amplitude decreases, the signal which is blurred by noise in the wireless channel, gets closer to the decision boundary making it increasingly vulnerable. With more sources, the peak to average ratio of the composite signal envelope increases and the problem gets worse, as we will see in Section 4.

2.2 Hardware

The oscillator's frequency accuracy of IEEE 802.15.4 compliant radios is mandated below $\pm 40\,\mathrm{ppm}$ [12]. This accuracy ensures tight bounds on the transmitter carrier frequency and allows the receiver to use a narrow channel filter to attenuate out-of-band noise power. However, a frequency discrepancy of up to 200 kHz is possible between two radios operating in the same channel of the 2.4 GHz band. We examine the carrier frequency dispersion for TelosB sensor nodes [14] employing a Software Defined Radio (SDR) from Ettus Research [7] for spectrum analysis, and an Agilent 8648C Signal Generator as a reference (10 Hz accuracy and time-base stability below $\pm 0.1\,\mathrm{ppm}$ typical). We verify such a frequency offset among nodes and observe no perceptible time variation in the frequencies, provided a constant room temperature is maintained.

The IEEE 802.15.4 standard also specifies the receiver sensitivity must be measured at a packet error rate (PER) of 1% for 52-symbol packets [12]. Thus, the required SER results near 10^{-4}, which we use as the reference threshold for minimal link performance. Note that a corresponding CER value, assuming chip errors are i.i.d., is not applicable since errors are more probable during envelope depressions. Hence, we measure both chip and symbol errors rates (CER and SER).

2.3 The Composite Channel

The signals traversing the wireless channel reach the receiver with amplitudes that depend on the path loss of the individual channels. Since the baseband signals are time synchronised, the receiver always locks with the preamble of the strongest signal (to decode the symbols). Therefore, when the amplitude imbalance is sufficiently large there

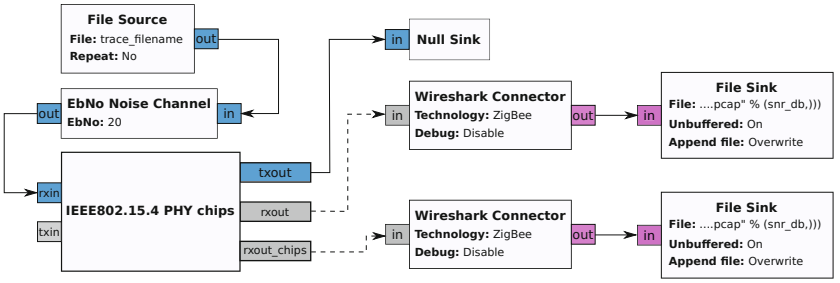

Fig. 1. GNU Radio flow graph used to measure SER and CER in the composite channel by adding synthetic noise in an AWGN channel

is always *capture*. However, when the magnitudes of the carriers are similar, intrinsic properties of the composite channel emerge.

The indoor multipath wireless channel is a time-invariant channel whose Channel Impulse Response (CIR) is considered quasistationary with a typical *rms delay spread* $\sigma_\tau < 100$ ns (see Saleh and Valenzuela [16]). Thus, the time dispersive nature of the channel is minimal and the coherence bandwidth is larger than the IEEE 802.15.4 Direct Sequence Spread Spectrum (DSSS) signal bandwidth. Also the individual channel is very slow time varying [16], with a coherence time much larger than the symbol duration, $T_{ci} \gg T_s$. This regime is known as *flat* and *slow* fading [11].

On the other hand, according to equation 2, the worst-case coherence time of the composite channel can be expressed as $T_{cc} = \pi/2w_c$ and results in $1\,\text{ms} \geq T_{cc} \geq 5\,\mu\text{s}$ with high probability, which is orders of magnitude shorter than what would be observed due to the Doppler spread. Thus, the composite channel one observes under CBI displays *fast* fading, which originates in the carrier frequency disparity of the participating repeater nodes.

3 Experimental Setup

We design our experiments to analyse the IEEE 802.15.4 PHY signals. This analysis benefits from an SDR platform as one can tap into the digital signal processing chain with ease. Our setup is designed around the Ettus USRP B210 board [7] and an SDR transceiver implementation in GNU Radio by Bloessl et al., which interoperates with IEEE 802.15.4 radios [1].

We employ a set of TelosB sensor nodes running Glossy [9] in a one-hop network composed of the initiator and at most eight repeaters. We then record low-noise complex baseband signals, at least 40 dB over the noise floor. We use an example application (`rx_sample_to_file`) from the USRP Hardware Driver (UHD) package running in an overdimensioned Linux workstation to avoid buffer overflows when recording the signal at $4\,\text{Msps}$. The initiator sends 15 packets per second, which are retransmitted 16 and 8 times for the wired and wireless experiments, respectively. Our 480-second-long baseband traces contain at least 1.6×10^5 symbols for our error-rate study. Note that failure to detect the PHY header invalidates the packet, thus we use payloads smaller than 16 byte to maintain robust statistics under high noise levels.

Our first configuration requires all antenna ports (from nodes and SDR) be wired through a 5-port 40 dB T-Network resistive power attenuator which acts as an ideal

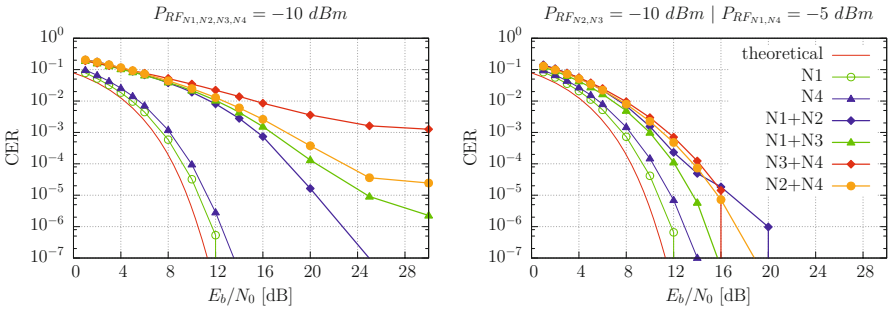

Fig. 2. The CER for pairs of nodes decreases for a 5-dB RF power imbalance. Each point in the graph is computed from 9.4×10^4 frames, 16 byte each. A 40-dB power attenuator fixes path loss to resemble a non-delay and non-multipath channel. Some curves were removed for clarity.

wireless channel without multipath distortions nor external interference. One node functions as the flooding initiator, transmitting at an RF power of $P_{RF} = -15$ dBm. Its signal runs through an additional 30-dB attenuator, thus reaching the SDR at -85 dBm. The repeater operates up to $P_{RF} = -5$ dBm, hence it reaches the SDR at -45 dBm. This power allocation is intended to guarantee the repeaters get the initiator packets with high probability but also forces its signal below the noise floor at the SDR.

Our second configuration involves a setup of sensor nodes fastened to an external glass wall, and the B210 SDR board with a 12-dBi YAGI antenna (ANT2400Y12WRU) fixed to a mast on the other end of the office, approximately 7 meters apart. In this case the initiator antenna is replaced with a dummy load to attenuate its signal.

The rest of our experiments are conducted off-line, in the computer, employing the rich component tool set in GNU Radio [10]. Using predefined payloads in Glossy, which are not altered by repeaters, we compute CER and SER by comparing the received frame content from the traces with the expected payload.

We extend the SDR transceiver by Bloessl et al. to export frames containing received chips, prior to decoding DSSS symbols. We generate two separate *packet capture* (pcap) files with frames containing chips and symbols respectively. In order to study link performance, we develop a channel module suitable to add controlled noise quantities to match a desired SNR value. This module requires specifying the energy-per-bit (E_b) to spectral noise density (N_0) ratio $^{Eb}/_{No}$ (in dB) and simulates an Additive White Gaussian Noise (AWGN) channel. The variance values σ^2 are internally computed based on the signal's peak amplitude, the bandwidth of the IEEE 802.15.4 channel and the specified $^{Eb}/_{No}$. By adding synthetic noise we can study a wide range of SNR ratios in a controlled and repeatable experiment. The GNU Radio flow graph used for the error-rate study is shown in figure 1. The flow graph consists of a file source, containing the complex baseband signal, our channel module to add Gaussian noise, and the extended transceiver. Frames containing decoded chips and symbols are stored in their respective pcap files for further processing.

4 Experimental Results

The IEEE 802.15.4 PHY coding scheme for the 2.4 GHz band uses pseudo-orthogonal codes where $k = 4$ bits are encoded together into an $n = 32$ chip sequence. The raw

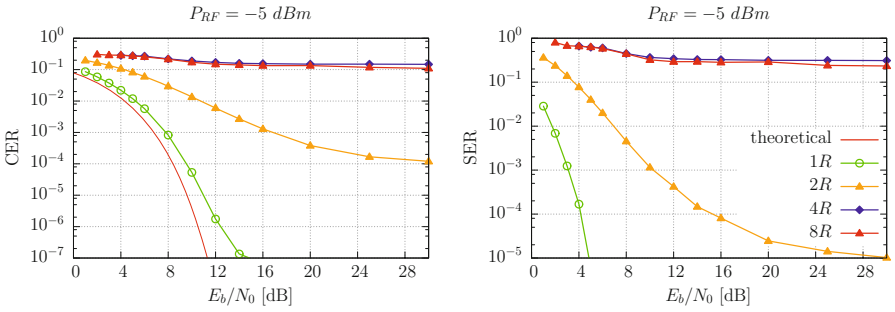

Fig. 3. CBI among up to eight repeater nodes after symbols traverse a highly correlated indoor wireless channel. Each point in the graph is computed from 4.8×10^4 frames, 8 byte each. The theoretical curve, as derived in [11, Section 6.1.2], is shown for CER only.

signalling is carried out using Offset-Quadrature-Phase-Shift-Keying with half-sine-shaping (OQPSK-HSS) at a rate of $2\,{}^{\text{Mchip}}/_{\text{s}}$. The code rate $r = {}^{k}/_{n} = {}^{1}/_{8}$ then results in a throughput of $250\,\text{kbps}$. Thus, DSSS processing gain is $P_G = 10\log(\frac{1}{r}) \approx 9\,\text{dB}$.

Since symbols are encoded in phase, magnitude variations of the signal do not directly impact detection reliability. However, as intersymbol distances in the constellation diagram diminish with the carrier amplitude, the envelope depressions lead to errors (Section 2.1). A brief summary of the most significant experimental results we have accumulated follows, illustrating the limits of the link performance under CBI.

4.1 Wired Configuration

We use a combination of up to three nodes directly *wired* to the SDR. This guarantees controlled and repeatable settings, as well as very similar power levels from repeaters. Additionally, the attenuator introduces a constant power loss across the signal bandwidth and proper impedance matching avoids reflections.

Figure 2 shows CER curves for single- and two-repeater combinations. All three-node combinations produce error rates well above 10^{-1} and are not shown. For pairs of nodes, we obtain a family of curves with varied and generally poor link performance. We observe a correlation between error rate and power (P_{RF}) imbalance. We show two power configurations: (i) all repeaters use $P_{RF} = -5$ dBm and (ii) decrease one repeater to $P_{RF} = -10$ dBm. As we raise the power imbalance by 5 dB, the link performance increases. Note that 5 dBm is the minimum power step the nodes allow.

The figure also shows that power imbalance moves the curves towards the minimum theoretically attainable error rate and near the single-repeater curve. We can relate this result with the ameliorated beating effect brought about by power imbalances. Note that having different amplitudes in equation (2) is better than having similar ones.

4.2 Wireless Configuration

We assess to what extent channel diversity could help reduce error rates. Figure 3 shows CER and SER for up to eight repeaters. For the two-node curve an ${}^{E_b}/_{N_0}$ of 16 dB is needed to maintain a minimum SER of 10^{-4}, a 12 dB difference relative to one repeater. For the cases of four and eight repeaters, both error rates remain above 10^{-1}.

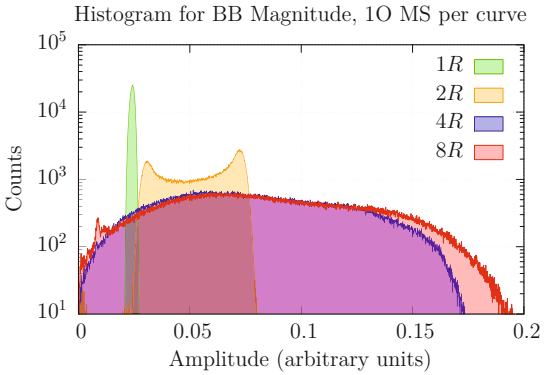

Fig. 4. Amplitude observations in the magnitude of the signal spread as the number of repeaters increases. Although the magnitude contains no information, the lower-end observations become vulnerable to noise, compromising link quality.

This experimental result indicates the channel diversity gain is limited for highly correlated indoor wireless channels. Unfortunately, these are very common settings for wireless sensor network deployments.

Furthermore, we estimate the *pdf* of the baseband signal's envelope. The results are shown in figure 4. As the number of repeaters increases, the envelope's histogram spreads, showing a large range of amplitude observations. Besides making the signal vulnerable to noise as previously discussed, the composite signal demands a high dynamic range on the receiver. As there is not an automatic gain control (AGC) on the B210 board, signal clipping may occur as more repeaters are added. We make sure the SDR operates in linear mode, hence the large error rates in figure 3 are exclusively due to the depressions in the composite signal. Note that the two-repeater curve in figure 4 recreates the behaviour described by equation (2). The rate of change of the cosine function that describes the envelope's undulations is lower on the extreme values, which explains the two peaks in the histogram.

5 Discussion and Conclusion

We have shown that link quality under CBI does not scale with the number of repeaters due to lack of coherence among multisource carriers. Specifically, the link layer reliability is affected by emerging fast fading in the composite channel, wherever capture effect is absent. Thus, we find a fundamental limitation that potentially impacts all concurrent transmissions and puts a high demand for dynamic range in the receivers. Commercial transceiver chip implementations feature greater receiver sensitivity than the SDR board used in these experiments, and use an AGC that reacts to (not very fast) envelope depressions by increasing the gain in the receiver's signal chain. Combined, these attributes can improve the apparent link quality, e.g. [9, figure 12]. However, we suspect this is effective for a low-noise channel only, since amplification cannot improve SNR.

Doddavenkatappa et al. orchestrate multichannel transmissions to sustain a packet pipeline while flooding the network [3,4]. Multichannel operation expands the degrees of freedom and time diversity increases probability of reception, but open questions remain in regard to suitable repeater selection for effective network flooding, i.e., guaran-

teeing power imbalance in all receivers, for enhanced performance. An alternative solution is to introduce channel diversity gain in the PHY layer, using space-time codes [13] which would be suitable for low-power design.

Acknowledgements. This work was partially supported by National Funds through FCT (Portuguese Foundation for Science and Technology) and by ERDF (European Regional Development Fund) through COMPETE (Operational Programme 'Thematic Factors of Competitiveness'); within projects PEst-OE/EEI/UI0319/2014, FCOMP-01-0124-FEDER-014922 (MASQOTS) and FCOMP-01-0124-FEDER-037281 (CISTER). We wish to thank Fernando A. Miranda Bonomi (National University of Tucumán, Argentina), for fruitful discussions and early contributions to this work during the ICTP School on Applications of Open Spectrum and White Spaces Technologies.

References

1. Bloessl, B., Leitner, C., Dressler, F., Sommer, C.: A GNU Radio-based IEEE 802.15. 4 Testbed. 12. GI/ITG FACHGESPRÄCH SENSORNETZE (2013)
2. Chebrolu, K., Raman, B., Mishra, N., Valiveti, P.K., Kumar, R.: Brimon: A sensor network system for railway bridge monitoring. In: ACM MobiSys, NY, USA (2008)
3. Doddavenkatappa, M., Chan, M.C., Leong, B.: Splash: Fast data dissemination with constructive interference in wireless sensor networks. In: USENIX NSDI 2013, Lombard, IL (2013)
4. Doddavenkatappa, M., Choon, M.: P3: A practical packet pipeline using synchronous transmissions for sensor networks. In: ACM/IEEE IPSN (2014)
5. Dutta, A., Saha, D., Grunwald, D., Sicker, D.: SMACK: A SMart ACKnowledgment scheme for broadcast messages in WLANs. In: ACM SIGCOMM, NY, USA (2009)
6. Dutta, P., Dawson-Haggerty, S., Chen, Y., Liang, C.J.M., Terzis, A.: Design and evaluation of a versatile and efficient receiver-initiated link layer for low-power wireless. In: ACM SenSys, Zurich, Switzerland (2010)
7. Ettus Research: USRP B200/B210 Bus Series Product Overview, `http://goo.gl/W0YLmQ`, (accessed: September 22, 2014)
8. Ferrari, F., Zimmerling, M., Mottola, L., Thiele, L.: Low-power wireless bus. In: SenSys. ACM, New York (2012)
9. Ferrari, F., Zimmerling, M., Thiele, L., Saukh, O.: Efficient Network Flooding and Time Synchronization with Glossy. In: ACM/IEEE IPSN, Chicago, IL, USA (April 2011)
10. GNU Radio Website, `http://www.gnuradio.org` (accessed September 2014)
11. Goldsmith, A.: Wireless Communications. Cambridge Univ. Press, NY (2005)
12. IEEE 802.15.4 Working Group: Wireless MAC and PHY Specs for Low-Rate WPANs, rev. 802.15.4-2011 edn. (September 2011)
13. Jafarkhani, H.: A quasi-orthogonal space-time block code. IEEE Transactions on Communications 49(1) (January 2001)
14. Polastre, J., Szewczyk, R., Culler, D.: Telos: Enabling ultra-low power wireless research. In: ACM/IEEE IPSN, Piscataway, NJ, USA (2005)
15. Rahul, H., Hassanieh, H., Katabi, D.: SourceSync: A Distributed Wireless Architecture for Exploiting Sender Diversity. In: ACM SIGCOMM 2010, New Delhi, India (August 2010)
16. Saleh, A.A.M., Valenzuela, R.: A statistical model for indoor multipath propagation. IEEE Journal on Selected Areas in Communications 5(2), 128–137 (1987)
17. Wang, Y., He, Y., Mao, X., Liu, Y., Huang, Z., Li, X.Y.: Exploiting Constructive Interference for Scalable Flooding in Wireless Networks. In: IEEE INFOCOM, Orlando, FL, USA (2012)
18. Maghsoodi, Y., Exact, S.A.: amplitude distributions of sums of stochastic sinusoidals (2008)